Isolation and characterization of cellulose nanofibers from bamboo using microwave liquefaction combined with chemical treatment and ultrasonication

Jiulong Xie [a,c], Chung-Yun Hse [b], Cornelis F. De Hoop [c], Tingxing Hu [a], Jinqiu Qi [a,*], Todd F. Shupe [c]

[a] College of Forestry, Sichuan Agricultural University, Chengdu, Sichuan 611130, China
[b] Southern Research Station, USDA Forest Service, Pineville, LA 71360, USA
[c] School of Renewable Natural Resource, Louisiana State University Agricultural Center, Baton Rouge, LA 70803, USA

ARTICLE INFO

ABSTRACT

Cellulose nanofibers were successfully isolated from bamboo using microwave liquefaction combined with chemical treatment and ultrasonic nanofibrillation processes. The microwave liquefaction could eliminate almost all the lignin in bamboo, resulting in high cellulose content residues within 7 min, and the cellulose enriched residues could be readily purified by subsequent chemical treatments with lower chemical charging and quickly. The results of wet chemistry analyses, SEM images, and FTIR and X-ray spectra indicated the combination of microwave liquefaction and chemical treatment was significantly efficient in removing non-cellulosic compounds. Ultrasonication was used to separate the nanofibrils from the purified residues to extract nanofibers. The TEM images confirmed the presence of elementary fibrils, nano-sized fibril bundles, and aggregated fibril bundles. As evidenced by the TGA analysis, cellulose nanofibers isolated by this novel technique had high thermal stability indicating that the isolated nanofibers could possibly be applied as reinforcing elements in biomaterials.

© 2016 Elsevier Ltd. All rights reserved.

1. Introduction

Renewable and biodegradable lignocellulosic biomass is of great interest because of depleting fossil fuel reserves and increasing public concern for environmental stewardship. Cellulose is the main component of lignocellulosic biomass and has received increasing attention due to its wide existence, excellent performance, biocompatibility, low density, thermal stability, and environmental benefits (Fatah et al., 2014). Recently, cellulose has been considered as a promising resource for reinforcing polymer matrixes for the preparation of green sustainable materials and bioethanol production. Regardless of its potential applications in emerging bio-based materials and bioenergy industries, cellulose consists of a linear homopolysaccharide composed of β-D-glucopyranose units linked together by β-1-4-linkages (Khalil et al., 2014). The cellulose molecules are aggregated into elemental fibrils with diameter ranges of 2–5 nm by intermolecular forces and hydrogen bonds (Hideno, Abe, & Yano, 2014). Therefore, from its unique biological structure, it is reasonable that various nanometer sized single fibers that are also referred to as cellulose nanocrystals, whiskers, nanowhiskers, cellulose nanofibrils, microfibrillated cellulose, or nanofibers have been isolated (Khawas & Deka, 2016; Shinoda, Saito, Okita, & Isogai, 2012; Sacui et al., 2014; Wu et al., 2013; Yue et al., 2012).

With the growing demand for sustainable green materials, isolation of cellulose nanofibers has been extensively investigated (Khalil et al., 2014; Khalil, Bhat, & Yusra, 2012). Nanofibers have been widely used for the preparation of nanostructured biocomposites (Ansari, Skrifvars, & Berglund, 2015; Awal, Rana, & Sain, 2015; Silverio, Neto, Dantas, & Pasquini, 2013), tough hydrogels (Abe, Ifuku, Kawata, & Yano, 2014), membranes (Ma, Burger, Hsiao, & Chu, 2014), and transparent nanopaper or film (Qing et al., 2015; Sun, Wu, Ren, & Lei, 2015) owing to its high crystalline with strong mechanical performance and outstanding thermal stability (Tibolla, Pelissari, & Menegalli, 2014). Over the past decades, a large number of lignocellulosic biomass has been explored for the generation of cellulose nanofibers (Abe, Iwamoto, & Yano, 2007). The common raw materials used for the production of cellulose nanofibers are wood (Wang, Li, Yano, & Abe, 2014), bamboo (Lu, Lin et al., 2015), wheat straw (Chen et al., 2011), Phormium

tenax (Fortunati et al., 2013), banana peels (Khawas & Deka, 2016; Pelissari, Sobral, & Menegalli, 2014), orange peel waste (Hideno et al., 2014), date palm fruit stalks (Hassan, Bras, Hassan, Silard, & Mauret, 2014), oil palm empty fruit bunch (Fahma, Iwamoto, Hori, Iwata, & Takemura, 2010), de-pectinated sugar beet pulp (Li, Wang, Li, Cheng, & Adhikari, 2014).

Usually, pretreatment and nanofibrillation are essential processes for the isolation of cellulose nanofibers from plant fibers. The pretreatment process such as acid or alkali treatment (He, Jiang, Sun, & Xu, 2014; Yue et al., 2015), enzymatic pretreatment (Hassan, Bras, Hassan, Silard, & Mauret, 2014; Tibolla et al., 2014; Zhu, Sabo, & Luo, 2011), ionic liquids (Han, Zhou, French, Han, & Wu, 2013), TEMPO (2,2,6,6-tetramethylpiperidine-1-oxyl) mediated oxidation (Jausovec, Vogrincic, & Kokol, 2015; Shimizu, Saito, & Isogai, 2014; Takaichi, Saito, Tanaka, & Isogai, 2014), and steam explosion treatment (Chirayil et al., 2014) were first used to remove non-cellulosic materials in plants, and then nanofibrillation technologies such as grinders (Jang, Lee, Endo, & Kim, 2013; Yousefi et al., 2013), high-pressure homogenizers (Yue et al., 2012), and ultrasonic method (Tang, Yang, Zhang, & Zhang, 2014) were used to generate high shear forces to separate the fibrils from the purified cellulose fibers.

Though cellulose nanofibers have been successfully isolated from these aforementioned technologies and the results were encouraging, drawbacks still exist such as chemical regent cost, high energy consumption, time-consuming, and equipment degradation has limited these techniques for practical applications. Advanced techniques for production of cellulose nanofibers with low cost, environmentally friendly, and time efficiency are still required.

As an efficient method, liquefaction has been applied in the conversion of solid woody materials into soluble liquid products, and the liquid products have shown great potential as alternatives for petroleum to produce value-added bio-based products (Xie, Qi, Hse, & Shupe, 2014). In recent years, microwave energy has been applied in the liquefaction of lignocellulosic biomass to enhance the biomaterials industry (Xie, Hse, Shupe, Qi, & Pan, 2014; Xie, Zhai, Hse, Shupe, & Pan, 2015). Compared to conventional liquefaction, microwave-assisted liquefaction has advantages such as time efficiency, low chemicals and energy consumption, and economically viability. The products from this technique also showed comparable properties compared to the commercialized ones. As for the liquefaction of wood residues in the binary of glycerol and ethylene glycerol, lignin and hemicellulose in the wood were significantly decomposed in the initial liquefaction stage (20–40 min) with the reaction temperature of 160 °C, while the cellulose content in the wood increased (Zhang, Pang, Shi, Fu, & Liao, 2012). Pan also observed that the lignin content in the liquefied Chinese tallow wood residue significantly decreased as the liquefaction processes resulting in enriched cellulose residues (Pan, Shupe, & Hse, 2007). The lignin content in the microwave liquefied bamboo residues also showed significantly decrease as the reaction temperature increased from 75 °C to 120 °C (Xie, Hse et al., 2014). Therefore, it could be concluded that in the reactions of both conventional and microwave-assisted liquefaction of lignocellulosic biomass in an organic solvent with acid as a catalyst, the decomposition of the three major components (cellulose, lignin, and hemicellulose) in lignocellulosic biomass was in the order of lignin, hemicellulose, and cellulose.

Based on this mechanism, Chen proposed a selective liquefaction process for the production of cellulose and biobased resins, the finding in his research showed that large amount of hemicellulose and lignin could be liquefied at 100 °C in 30 min, and the retained cellulose had higher susceptibility for enzymatic attack. This approach offered a new approach for the utilizations of lignocellulosic biomass in the bioethanol and biobased materials industries (Chen, Zhang, & Xie, 2012). In order to extract cellulose

for use in both bio-fuels and reinforcing materials, the combination of bleach and liquefaction processes was described in the research of Li et al. (2015), in which hemicellulose was selectively liquefied to get cellulose. From the previous research results, it was obvious that cellulosic fibers could be easily produced by subjecting the raw lignocellulosic biomass to a liquefaction process with reactions conditions properly controlled.

Therefore, in this study microwave liquefaction was proposed to generate cellulose enriched residues from bamboo. Thereafter, the cellulose enriched residues were chemically purified with low charging of chemicals. Cellulose nanofibers were isolated by ultrasonic nanofibrillation of the chemically purified cellulose fibers. Morphology, crystallinity, and thermal stability of the isolated nanofibers were determined by employing scanning electron microscopy, X-ray diffraction, and thermogravimetry, respectively. This study attempts to achieve an efficient approach for the generation of cellulose nanofibers with the combination of microwave liquefaction and ultrasonic nanofibrillation.

2. Materials and methods

The major procedures for isolation of nanofiber in this study included reduction of bamboo, microwave liquefaction, anti-solvent fractionation, chemical treatments, and ultrasonication. Fig. 1 depicts the flow chart of the procedures.

2.1. Materials

Three-year-old moso bamboo culms (*Phyllostachys pubescens*) were harvested from the Kisatchie National Forest, Pineville, La, USA. The moso bamboo was selected because the annual yield of moso bamboo was greater than all other kinds of bamboo (about 1.8×10^7 tons) and the integrated utilizations of moso bamboo via liquefaction may provide potential approach for the production of high-value added bioproducts (Jiang et al., 2012). The bamboo culms were reduced to particles using a Thomas Wiley Laboratory Mill (Model 4) equipped with a 2 mm screen. The particles (length: 0.05–6.23 mm, diameter: 0.01–1.1 mm) were screened to collect particles that passed through a 20-mesh sieve and then retained on a 40-mesh sieve. The average length and diameter of the particles of 20–40 mesh were 5.06 mm and 0.567 mm, respectively. The weight percentage of particles between 20 mesh and 40 mesh was 25.20%, and that for particles in the range of 10–20 mesh, 40–60 mesh, 60–80 mesh, 80–100 mesh, and >100 mesh were 0.22%, 44.42%, 10.08%, 5.86%, and 14.22%, respectively. The particles were dried to a constant weight in an oven maintained at 80 °C. The dried particles were stored in polyethylene bags and used without further treatment. All chemicals including acids, glycerol, and methanol were of reagent grade and obtained from commercial sources.

2.2. Microwave liquefaction

Microwave liquefaction of bamboo was carried out in a Milestone laboratory microwave oven (Ethos EX, 1200 W maximum microwave power, 100 bar maximum operating pressure, ASM-400 magnetic stirrer for homogenous mixing of samples, 300 °C maximum operating temperature, fiber-optic temperature sensor) equipped with 100 mL sealed Teflon reaction vessels that are actually a system of components that consist of a vessel that contains the sample, a vessel cover, a safety shield, a vent indicator ring, and a pressure adapter plate. The Teflon vessels used in this study have excellent properties with regard to temperature, acid, and pressure resistance, which was suitable for the chemicals used in this research. The application of this vessel system also enables that the microwave system could provide a closed, clean environment, pre-
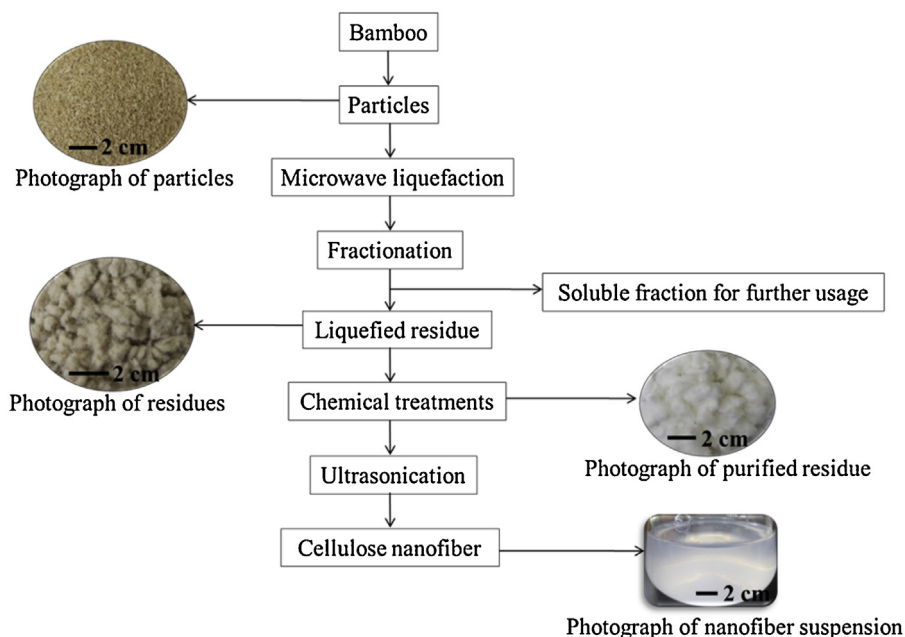
Fig. 1. Procedures for the isolation of cellulose nanofibers in this study.(For interpretation of the references to color in the text, the reader is referred to the web version of this article.)

vent loss of volatile species, minimize the use of expensive acids, and safely release the over-pressures in the vessel.

Mixed glycerol and methanol at a ratio of 2/1 (w/w) were used as the solvent at a solvent to bamboo ratio of 4/1 (w/w). Sulfuric acid (1.75% of solvent weight) of concentration of 98% (wt) was used as the catalyst because sulfuric acid could provide strong acid sites during the liquefaction reaction. The highly reactive protons in sulfuric acid are able to activate the oxygen atoms in the glycosidic bonds. The reaction mixture consisting of 2 g of bamboo particles, 8 g of solvent, and 0.14 g of sulfuric acid were loaded in 100 mL Teflon vessels with a magnetic stirring bar. The Teflon vessels were then placed on the rotor tray inside the microwave cavity. The temperature was increased from room temperature to 120 °C in 3 min and then was kept constant for a desired time. The temperature was monitored using an ATC-400FO automatic fiber optic temperature control system by putting the sensor into a reference vessel. As for the reaction setup in this study, microwave power was automatically adjusted in the range of 0–550 W based on continuous feedback from the process sensors to allow the reaction to follow the desired temperature profile. At the end of the reaction, the vessels were removed from the microwave cavity and cooled for 15 min. Afterwards, the resulting reaction mixtures were dissolved in methanol and then vacuum-filtered through Whatman No. 4 filter paper. The solid retained on the filter paper was washed with methanol and oven-dried at 105 °C. The yield is the mass percentage of the residue solid to the original bamboo.

2.3. Chemical treatments

The residues from the microwave liquefaction process were further chemically purified. The residues were first bleached in acidified NaClO$_2$ solution (0.1% w/v) at 75 °C for 1 h. The bleaching process was to remove the phenolic compounds or molecules from lignin retained in the residues after microwave liquefaction. The residue was filtered and washed with deionized water until its pH was neutral. Next, the beached residues were treated with NaOH solution (0.4%) at 75 °C for 30 min to partially remove hemicellulose. Thereafter, the residual was filtered and rinsed with deionized water until the pulp was neutral.

2.4. Ultrasonic nanofibrillation

The chemically purified residues were soaked in deionized water (concentration 0.2 wt%) and then subjected to ultrasonic fibrillation using an ultrasonic generator equipped with a 1.5 cm cylindrical probe. The process was performed at a frequency of 25 kHz with an output power of 750 W for 30 min. The ultrasonic fibrillation was conducted in an ice bath, and the ice was maintained throughout the entire process.

2.5. Characterization

2.5.1. Cellulose content
The purity of the fibers from each stage was characterized by determination of α-cellulose content in accordance with ASTM D 1102-84. The residual lignin content was determined by the Klason lignin method (ASTM D 1106-96). A referenced method was used to determine the hemicellulose content (Zhang, Pang, Shi, Fu, & Liao, 2012).

2.5.2. Scanning electron microscope
The surface morphology of the bamboo particles and fiber samples were observed using scanning electron microscopy (SEM, JCM-5000). Test samples were coated with gold using a vacuum sputter coater before subjected to the SEM analysis.

2.5.3. Transmission electron microscope
The concentration of aqueous cellulose nanofibers suspensions was diluted from 0.2% to 0.01% (w/w). A droplet of the diluted suspension was deposited on the surface of carbon-coated copper grids. As for contrast in TEM, the cellulose nanofibers were negatively stained in a 2% (wt) solution of uranyl acetate. The morphology of cellulose nanofiber was observed using a transmission electron microscope (TEM, JEOL 100CX, JEOL, Inc., Peabody, MA, USA) with an accelerating voltage of 80 kV. The diameter of the cellulose nanofibers were calculated by measuring one hundred fibers randomly selected from several TEM images.

2.5.4. Fourier transform infrared spectroscopy

The FT-IR analysis was performed by a Nicolet Nexus 670 spectrometer equipped with a Thermo Nicolet Golden Gate MKII Single Reflection ATR accessory. Data collection was performed with a 4 cm^{-1} spectral resolution and 32 scans were taken per sample.

2.5.5. X-ray diffraction

Crystallinity of the original bamboo and fiber samples were analyzed using wide angle X-ray diffraction (Bruker D 5000). The data were generated by a diffractormeter with Cu Kα radiation (λ = 1.54 A) at 40 kV and 30 mA over the angular range 2θ = 5–40° and a step time of 2.0 s. A focusing powder diffraction method was applied. The crystallinity index (CrI) was determined using the following equation:

$$CrI(\%) = \frac{I_{002} - I_{am}}{I_{002}} \times 100 \qquad (1)$$

where I_{002} is the intensity of the diffraction from the (200) plane at 2θ = 22.1°, and I_{am} is the intensity for amorphous material taken at 2θ = 18° (French, 2014).

2.5.6. Thermogravimetric analysis

TG/DTG analysis was conducted with a thermal analyzer, TGA (Q50), to simultaneously obtain thermogravimetric data. About 2 mg of sample was analyzed by the thermal analyzer. Pyrolysis was terminated at 800 °C with a heating rate of 20 °C/min under a flow of 60 mL/min of nitrogen gas.

3. Results and discussion

3.1. Liquefaction and preparation of cellulose fibers

Cellulose fibers were isolated by the combination of a microwave liquefaction process combined with bleaching and alkali treatment prior to subjecting to ultrasonic nanofribillation. Table 1 illustrates the yield and chemical compositions of the residues after the microwave liquefaction and chemical treatment stages. The residue yield decreased with increasing reaction time. The residual lignin content in the liquefied residues showed a significant decrease with respect to reaction time, while the cellulose content significantly increased. Table 1 also indicated that the liquefaction of bamboo could also partially eliminate the hemicellulose. However, the hemicellulose content first increased and then decreased with increasing liquefaction time. The increase in hemicellulose content in the initial reaction stage was attributed to the significant weight loss of lignin, and thereafter enriched the residue resulting in higher (relatively) cellulose and hemicellulose content, and the decrease in hemicellulose as the liquefaction processing was mainly due to the degradation of hemicellulose itself. The decrease in residue yield induced by prolonging the reaction time is mainly due to the efficient removal of non-cellulosic components such as lignin and hemicellulose from bamboo, and thus resulting in the increase in cellulose content. The residues obtained from the liquefaction at 120 °C/7 min had a cellulose content of 70.74%, which was about 170% of that for the original bamboo, and the residual lignin content was as low as 1.66%.

However, the residues with high cellulose content from the liquefaction process at 120 °C/7 min showed a light brownish color (Fig. 1), indicating that a small amount of lignin was retained in the residue as confirmed by the above mentioned chemical analysis results. To further purify the fibers from the liquefaction process at 120 °C/7 min, chemical treatments were conducted in sodium chlorite and alkali solution (0.4%). After chemical treatment, the residues became pure white, and the cellulose content increased to 83.67%, and the lignin content was as low as 0.13%. The chemically

purified residues obtained in this study showed comparable cellulose content as that reported in Chen's report (Chen et al., 2011), i.e., α-cellulose content for chemically purified bamboo fiber was 84.4%. Moreover the time required for such purity of cellulose fibers was mere 1/8 of that in Chen's study. Chemically purified cellulose as reported in Chen's study was obtained from a process involving dewaxing, bleaching, alkali treatment in 16 h. Furthermore, after liquefaction, the chemical usage for further purifying residues was much lower than that used in previously reported methods (Wu et al., 2013), in which dewaxed samples were bleached three time in 1.4% acidified NaClO$_2$ followed by alkali treatment with 5% KOH for 4 h.

3.2. Morphological observation

SEM images of the raw bamboo particles and samples from microwave liquefaction and chemical treatments are presented in Fig. 2. The original bamboo showed large fiber bundles and intact structures. Some small fragments were attached on the uneven surfaces (Fig. 2a and b). The diameter of the raw bamboo sample was 567 ± 149 μm. The morphological structure of the residues from microwave liquefaction differed significantly from that of the original bamboo. After 7 min of reaction time, the fiber bundles were separated into individual micro-sized fibers with a diameter of 17 ± 6.9 μm. The separation of fasciculus induced by microwave liquefaction is mainly attributed to the removal of lignin in the middle lamella, resulting in the collapse of the compact bamboo structure. It was obvious that the microwave liquefaction was efficient in defibrillation of bamboo by dissociating and dissolving the cementing components. As can be seen in Fig. 2d, small granules (1–2 μm) were found on the surface of the residues. These granules were ascribed to lignin substrates. Similar granules were also observed on the residues from microwave liquefaction of bamboo for biopolyols, and the granules were confirmed as lignin substrates by FTIR analysis (Xie, Hse et al., 2014; Xie, Huang, Qi, Hse, & Shupe, 2014). This result indicated that a small amount of lignin was still retained on the residues, which was consistent with results from the wet chemistry analysis as discussed above.

After bleaching due to the complete elimination of lignin on the fiber surface and in the fiber cell wall, the micro-sized fibers were opened as evidenced by fissures (Fig. 2e). Meanwhile the fiber surface became rough, and microfibrils bundles (0.5–1.0 μm) that were composed of nano-sized fibrils were obviously visible and began to peel off from the micro-sized fibers (Fig. 2f). Compared to the fibers from the bleached residues, fibers from the alkali treated residues became irregular and were much rougher because of the partial removal of hemicellulose (Fig. 2g). Curled and flat fiber cells with many fibril bundles attached were observed in the SEM images of the alkali treated residues (Fig. 2g). From the SEM images of the alkali treated fibers, it seemed that the nano-sized fibril bundles attached to each other without any non-cellulosic cements filling in the space (Fig. 2h). The ultrasonic treatments resulted in the breakdown of the hydroxyl bonds and nano-sized fibril bundles and individual nano fibrils were released as evident from the TEM images.

The obtained cellulose nanofiber aqueous suspension was diluted and characterized by TEM. The TEM images confirmed the presence of individual nanofibers (Fig. 3a). As shown in Fig. 3b, individual long fiber-like nano fibrils were entangled together forming a web-like structure. An interconnected network of nanofibers could provide great reinforcing capability for composite applications (Bhatnagar & Sain, 2005); therefore, the nanofibers obtained in this study are of particular interest for future research in this regard. It is interesting to note that an opening of a fibril bundle (19 nm) is clearly shown in Fig. 3c. The diameters of the split single fibrils in the opening position were 2–5 nm, which was in the diam-
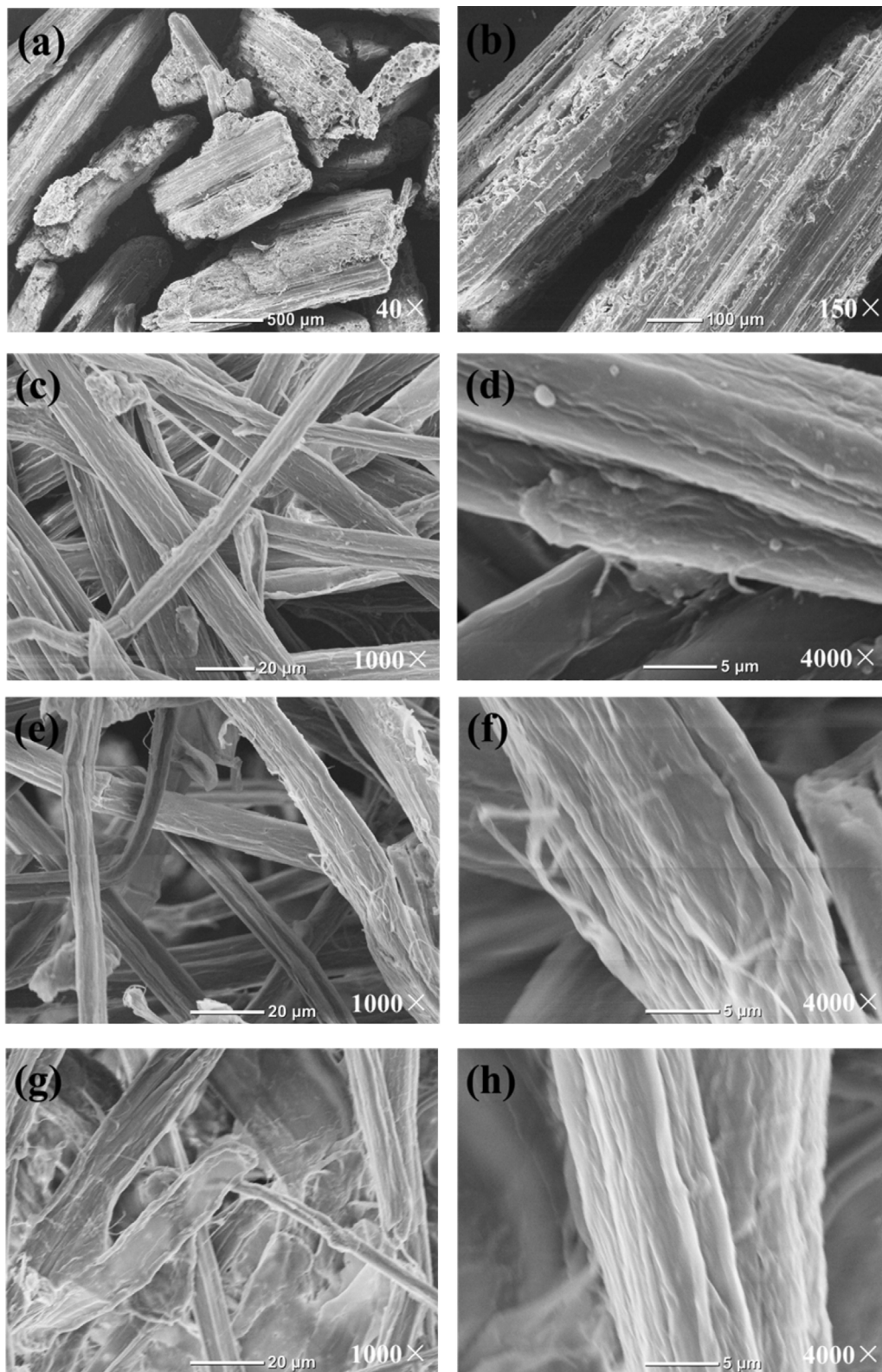
Fig. 2. SEM images of original bamboo (a and b), residue from microwave liquefaction of 120 °C/7 min (c and d), residue from the bleaching of liquefied residue (e and f), and residue from alkali treatment of bleached samples (g and h).

eter range of single elemental fibrils in higher plants (Somerville et al., 2004). This result demonstrated that the nanofribillation force introduced by the ultrasonicator was strong enough to defibrillate the cellulose fibers which were obtained by microwave liquefaction and chemical treatment to the elemental fibril level. This

was because ultrasonic treatment can break the hydrogen bonds and disintegrate microfibers into nanofibrils. Fig. 3d presents the aggregate of individual fibrils. It can be seen that individual fibrils associated with one another and formed a large aggregated bundle with a diameter of about 20 nm.
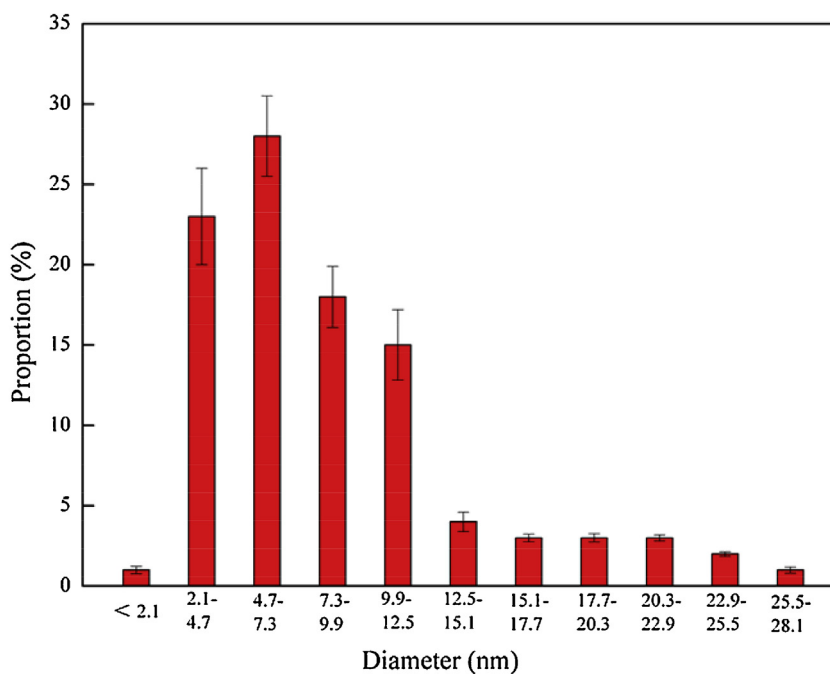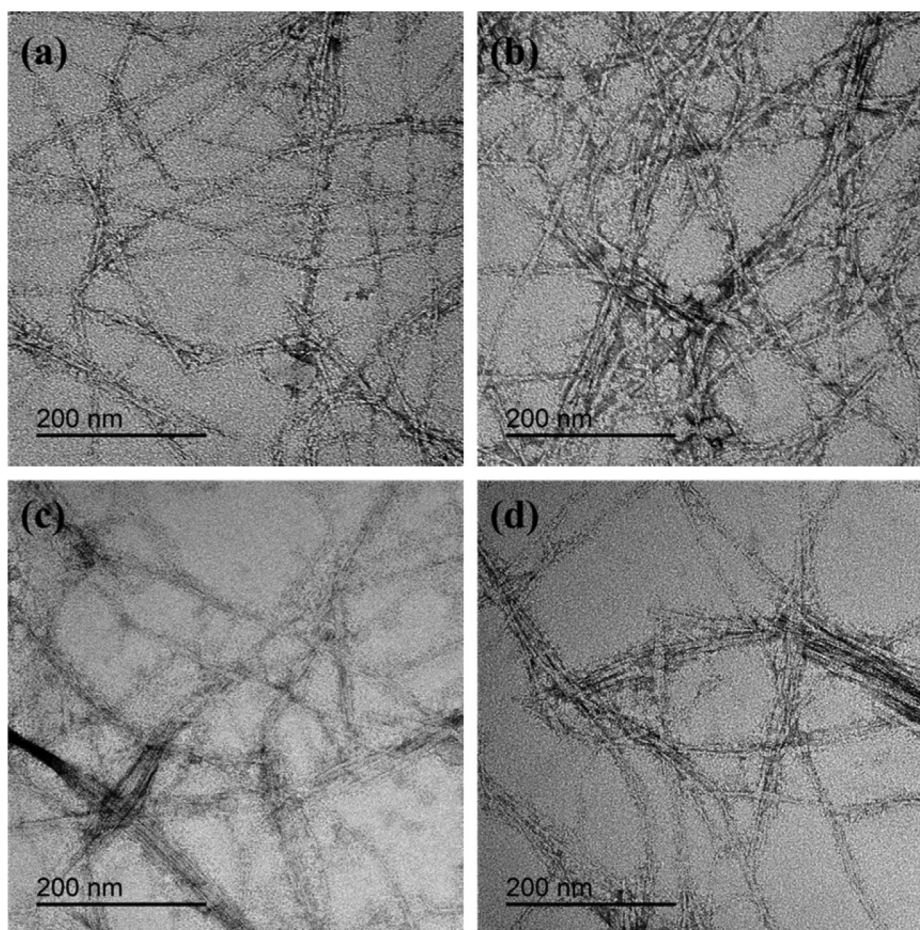
Fig. 3. TEM images of (a) individual/elemental fibril, (b) nanofiber network structure, (c) opening of fibril bundle, (d) aggregated bundle, and (e) diameter distribution.

The TEM images were further processed with analysis software (ImageJ) to determine the diameter. The diameter of the nanofibers was in the range of 2–30 nm. For comparison, the nanofibers obtained in this study had a similar diameter to the cellulose nanofibers isolated from bamboo in other studies; the diameter for nanofibers prepared by using mechanochemical and chemical-ultrasonic processes were 15–30 nm and 10–40 nm, respectively (Chen et al., 2011; Lu, Tang et al., 2015). Fig. 3e presents the

Table 1
Yield and chemical compositions of residues at each stage of the treatments.

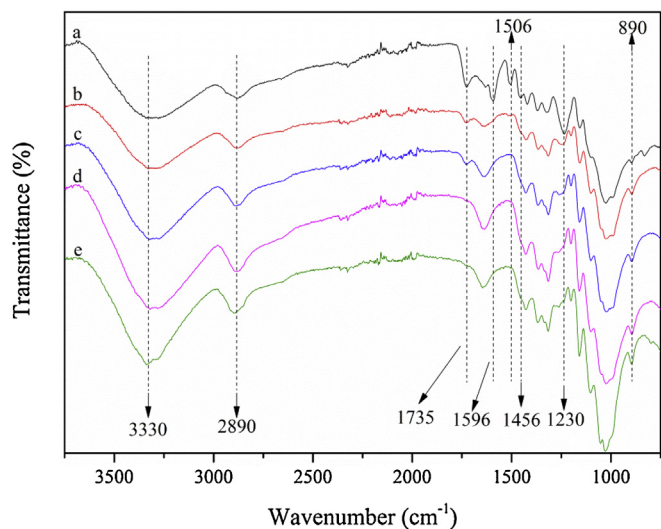| Samples	Residue yield (%)	Cellulose (%)	Hemicellulose (%)	Klason lignin (%)
Original bamboo	100.00 ± 0.00	41.72 ± 2.37	22.86 ± 2.19	20.91 ± 0.24
120 °C/3 min	60.95 ± 3.42	52.85 ± 3.16	25.49 ± 3.06	7.44 ± 0.61
120 °C/5 min	45.99 ± 1.87	66.74 ± 2.09	19.90 ± 1.58	3.82 ± 0.05
120 °C/7 min	42.28 ± 2.66	70.74 ± 1.78	18.85 ± 1.74	1.66 ± 0.15
Bleaching	37.51 ± 1.47	75.30 ± 1.31	18.53 ± 1.43	0.29 ± 0.02
Alkali treatment	34.17 ± 1.66	83.67 ± 2.69	13.97 ± 1.67	0.13 ± 0.06

Fig. 4. FTIR spectra of (a) original bamboo, (b) microwave liquefied residue, (c) bleached residue, (d) alkali treated residue, and (e) cellulose nanofiber.

diameter distribution of the nanofibers. About 70% of fibers have a diameter within 2–10 nm, 22% of the fibers had a diameter within 12–20 nm, and only 9% of the fibers had a diameter greater than 20 nm. The TEM images and the diameter distribution results revealed that the aqueous suspension contained nanometer scale fibers comprised of a large number of elemental fibrils, some fibril bundles, and a small amount of aggregated bundles.

There was no precipitate formed in the nanofiber aqueous suspension after setup for 24 h, indicating that the nanofiber samples were still stable after setup for 24 h (Fig. 1). This may be attributed to the strong fibrillation forces induced by high-intensity ultrasonication. The introduction of sulphate groups during the liquefaction process that was confirmed by the FTIR spectra as discussed later may also contribute to the stability of the nanofiber suspensions since the sulphate groups could provide negative electrostatic layer on the surface of the nanofibers resulting in the homogeneous and stable aqueous suspensions (Bondeson & Oksman, 2007).

3.3. FTIR spectroscopy analysis

The FTIR spectra of the original bamboo, microwave liquefied residue, bleached residue, alkali treated residue, and cellulose nanofiber are presented in Fig. 4. The absorbance peak at 3330 cm^{-1} represents the stretching vibration of OH and the intensity peak at 2890 cm^{-1} was attributed to the asymmetric stretching vibration of CH$_2$ in cellulose, hemicellulose, and lignin were found in all spectra.

The spectrum of the original bamboo showed a significant difference from that of the microwave liquefied residue. The peaks at 1735 cm^{-1} (attributed to the acetyl and uronic ester groups or the ester linkage of the carboxylic group of ferulic and *p*-coumaric acid of hemicellulose), 1596 cm^{-1} and 1506 cm^{-1} (arising from the aromatic skeletal vibration), 1456 cm^{-1} (assigned to C—H deformation combined with aromatic ring vibration), and 1230 cm^{-1}

(corresponding to methoxyl groups of lignin) were all shown to be strong peaks in the spectra of the original bamboo. The peak at 1735 cm^{-1} was weakened in the spectrum of microwave liquefied residue, indicating the cleavage of the linkages between ferulic acid or *p*-coumaric acid or (*p*-) hydroxycinnamic acids and lignin in the fibers (Sun & Chen, 2008). The dissociation of the key ester linkages between lignin and carbohydrates promoted the dissolution of lignin into the solvents. The absorbance bands at 1596 and 1456 cm^{-1} disappeared and the bands at 1506 and 1230 cm^{-1} became small shoulders. This result indicates that lignin functional groups such as aromatic rings were almost completely dissociated and dissolved with only a small amount of associated lignin retained on the residues. The retained lignin was confirmed by the aforementioned SEM images, in which lignin residues were observed on the exterior surface of the fibers from the residues. The absorbance band at 1203 cm^{-1} attributing to S=O vibration appeared in the spectra except for that of the original bamboo (Lu & Hsieh, 2010), revealing that sulphate groups were introduced during the microwave liquefaction process since sulfuric acid was used as the catalyst.

All of the four characteristic absorbance bands of lignin (1596, 1506, 1456, and 1230 cm^{-1}) were absent in the spectrum of the bleached residues (Fig. 4, spectrum c), suggesting the complete removal of lignin from the residue. The peak at 1735 cm^{-1}, attributed to hemicellulose, disappeared in the spectrum of the alkali treated residue. This disappearance indicated that the removal of hemicellulose was achieved by the diluted sodium hydroxide solution (Fig. 4, spectrum d). No significant difference was found between the spectra of the alkali treated residue and the nanofibers indicated that the ultrasonic nanofibrillation process did not change the chemical structures of the fibers.

3.4. Crystallinity analysis

Fig. 5 shows the WXRD spectra of the original bamboo, microwave liquefied residue, bleached residue, alkali treated residue, and cellulose nanofibers. All of the XRD patters displayed peaks at $2\theta = 14.9°$, $16.1°$, $22.1°$, and $34.5°$, corresponding to the $(1\bar{1}0)$, (110), (200), and (004) crystallographic planes, respectively (French, 2014). These peaks were typical signatures of cellulose I crystalline structure, which was performed by repeating β-$(1 \rightarrow 4)$ – D-glucopyranose units, and building blocks of parallel glucan chains (Paakko et al., 2007).

The calculated crystallinity index (CrI) values were 52.3 and 70.6% for the original bamboo and microwave liquefied residue, respectively. The bamboo crystallinity was improved by 135% after liquefying for 7 min. This significant increase ($p < 0.05$) of crystallinity in the microwave liquefied residues with comparison to the original bamboo was attributed to the efficient dissolution and removal of non-cellulosic materials such as lignin and extractives from the amorphous regions and enrichment in cellulose content in the liquefied residues during microwave liquefaction. This was in good agreement with the chemical analyses results (Table 1). This result also indicated that microwave liquefaction could be used as an efficient pre-purification process for the isolation of cellulose fibers.
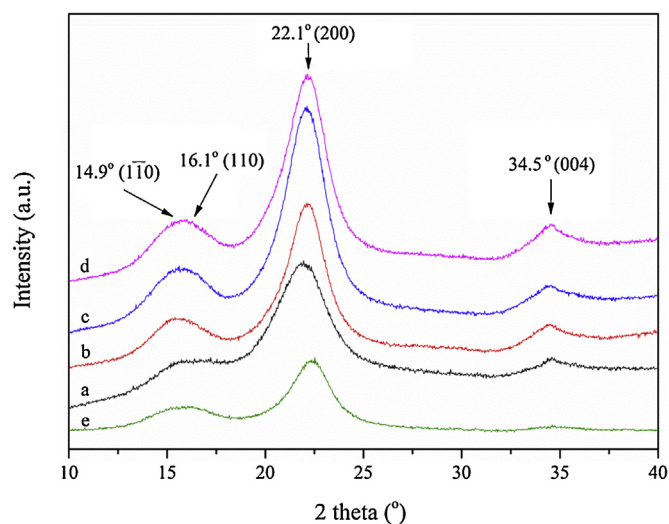
Fig. 5. X-ray diffraction spectra of (a) original bamboo, (b) microwave liquefied residue, (c) bleached residue, (d) alkali treated residue, and (e) cellulose nanofiber.

The crystallinity was further increased to 72.5% by the application of a bleaching treatment. This was mainly due to the complete elimination of retained lignin in the liquefied residues. The alkali treatment also improved the crystallinity of the bleached residue to 74.2% by partially removing the hemicellulose. However the crystallinity of the nanofibers was found to be lower than that for the alkali treated residue; the CrI for the nanofiber was 67.4%. This was likely due to the breakdown of the hydrogen bonds of the cellulose fibers during the ultrasonic nanofribillation process, revealing that the ultrasonication treatment caused damage to the crystalline domain of the nanofibers. This result was in accordance with a previous study in which Lu found that ultrasonication treatment could damage the crystalline region of cellulose resulting in a decrease in the crystallinity index (Lu, Tang et al., 2015). The decrease in the crystallinity for nanofibers from cellulose pulp was also reported when a high pressure homogenizer was applied for nanofribillation (Fatah et al., 2014).

3.5. Thermal stability

The TG and DTG curves of the original bamboo and samples from each stage are illustrated in Fig. 6. Three different weight loss processes were observed in the TG curve for the original bamboo. The initial weight loss was found in the temperature range of 50–200 °C due to the evaporation and removal of bound water and loss of extractives existing in bamboo (Qi, Xie, Hse, & Shupe, 2013). A dramatic weight loss was shown in the temperature range of 220–450 °C which was attributed to the thermal depolymerization of carbohydrates and lignin. The small weight loss in the temperature range of 450–650 °C contributed to the degradation of lignin residues from the second stage tar and char. On the DTG curve of the original bamboo, a small shoulder at 260 °C corresponding to the decomposition of hemicellulose was found. The peaks on the DTG curves were the maximum degradation rate temperature (T_{max}) corresponding to the thermal decomposition of cellulose and the T_{max} for the original bamboo was 333 °C.

The T_{max} for the microwave liquefied residue was 25 °C lower than that for the original bamboo. The reason may be that, the compact bamboo structure was dissociated by microwave liquefaction; the obtained residues had a larger surface area comprised of small hemicellulose and lignin fragments that could be easily decomposed at lower temperature (Pang, Gaddipatti, Tucker, Lester, & Wu, 2014). These substances may initiate more active
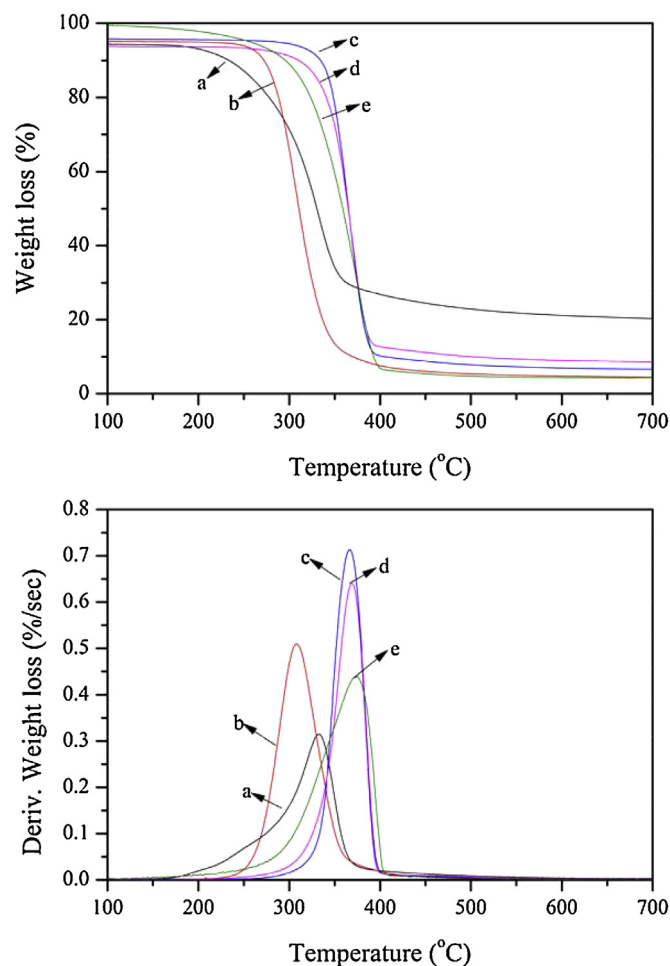

Fig. 6. TGA and DTG curves of (a) original bamboo, (b) microwave liquefied residue, (c) bleached residue, (d) alkali treated residue, and (e) cellulose nanofiber.

sites and accelerate the decomposition of the residues. Another explanation may be the introduction of sulphate groups into the residues during the liquefaction process, which was confirmed by the FTIR spectra as shown in Fig. 4 and discussed earlier. The sulphate groups worked as a dehydration catalyst and decreased the activation energy of cellulose chain degradation (Jahan, Saeed, He, & Ni, 2011). The bleached residue and alkali treated residue showed a higher T_{max} than the original bamboo. This was largely due to the complete elimination of lignin and partial removal of hemicellulose. The highest T_{max} was found for nanofiber, 374 °C. Meanwhile, the lowest char yield was obtained for the nanofiber, which was due to the removal of non-cellulosic components in the nanofibers. Similar results were found in the isolation of nanofibrils from the *Helicteres isora* plant (Chirayil et al., 2014). The thermogravimetric analysis revealed the nanofiber obtained in this study had high thermal stability.

3.6. Formation mechanism

A formation mechanism of cellulose nanofiber from bamboo was proposed based on the aforementioned results and analyses (Fig. 7). At the first step, the ester linkages between the carbohydrates and lignin were dissociated and lignin in the middle lamella was depolymerized by microwave liquefaction, which resulted in the dissociation of the intact raw bamboo into micro-sized residues. The microwave liquefied residues had considerable accessibility for subsequent chemical purification. Then, bleaching and alkali
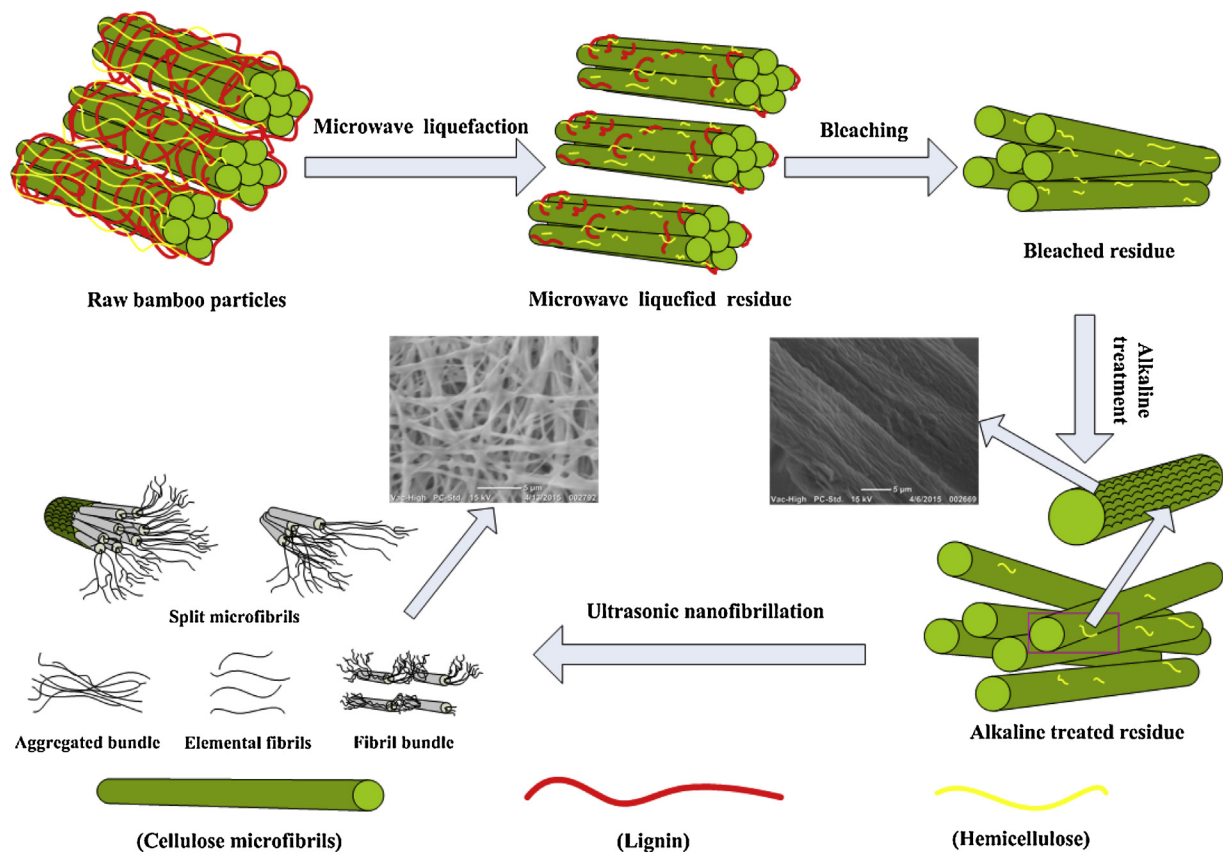
Fig. 7. Formation mechanism of cellulose nanofiber from bamboo via the combination of microwave liquefaction and ultrasonication process.

treatment were applied to completely eliminate the lignin and partially remove the hemicellulose in the residues, respectively. After alkali treatment, the cellulose fibers showed an irregular and rough morphology allowing it more accessible for physical force. Finally, ultrasonic radiation was used to break the hydrogen bonds. Therefore, element nano fibrils and nano fibril bundles were obtained. The microwave liquefaction process serves a prominent role in the purification and defibrillation of raw bamboo during the whole process since it enhanced the efficiency for subsequent operations by decreasing the chemical usage and time requirement.

4. Conclusions

The present work showed that cellulose nanofibers could be successfully extracted from bamboo with microwave liquefaction and chemical treatment as a purification process and ultrasonication as a nanofibrillation process. Bamboo bundles were converted into micro-sized fibers with high cellulose content by microwave liquefaction prior to chemical treatments. For the extraction of purified cellulose fibers, bleaching and alkali treatment were employed. However, the amount of chemical reagents and time required were 1/8 of that of traditional methods. Due to the complete elimination of lignin and partial removal of hemicellulose, the chemically purified residues took on an irregular and rough morphology and fibril bundles began to split off from the fiber framework. The presence of cellulose nanofibers were confirmed by TEM images, and the diameters of the nanofibers were in the range of 2–30 nm. FTIR and XRD spectra revealed that the combination of microwave liquefaction and chemical treatment was an efficient approach for removing non-cellulosic materials in bamboo for cellulose nanofibers production purpose. Ultrasonic irradiation resulted in a reduction in crystallinity of cellulose nanofibers. The isolated cellulose

nanofibers have potential application for the fabrication of thermally stable composites because of their high thermal stability. Based on these results, this new proposed method could be developed into a practical technique for the generation of cellulose nanofibers.

References

Abe, K., Iwamoto, S., & Yano, H. (2007). Obtaining cellulose nanofibers with uniform width of 15 nm from wood. *Biomacromolecules, 8*, 3276–3278.
Abe, K., Ifuku, S., Kawata, M., & Yano, H. (2014). Preparation of tough hydrogels based on β-chitin nanofibers via NaOH treatment. *Cellulose, 21*, 535–540.
Ansari, F., Skrifvars, M., & Berglund, L. (2015). Nanostructured biocomposites based on unsaturated polyester resin and a cellulose nanofiber network. *Composites Science and Technology, 117*, 298–306.
Awal, A., Rana, M., & Sain, M. (2015). Thermorheological and mechanical properties of cellulose reinforced PLA bio-composites. *Mechanics of Materials, 80*, 87–95.
Bhatnagar, A., & Sain, M. (2005). Processing of cellulose nanofiber-reinforced composites. *The Journal of Reinforced Plastics and Composites, 24*, 1259–1268.
Bondeson, D., & Oksman, K. (2007). Dispersion and characteristics of surfactant modified cellulose whiskers nanocomposites. *Composite Interfaces, 14*, 617–630.
Chen, W. S., Yu, H. P., Liu, Y. X., Hai, Y. F., Zhang, M. X., & Chen, P. (2011). Isolation and characterization of cellulose nanofibers from four plant cellulose fibers using a chemical-ultrasonic process. *Cellulose, 18*, 433–442.
Chen, H. Z., Zhang, Y. C., & Xie, S. P. (2012). Selective liquefaction of wheat straw in phenol and its fractionation. *Applied Biochemistry and Biotechnology, 167*, 250–258.
Chirayil, C. J., Joy, J., Mathew, L., Mozetic, M., Koetz, J., & Thomsa, S. (2014). Isolation and characterization of cellulose nanofibrils from *Helicteres isora* plant. *Industrial Crops and Products, 59*, 27–34.
Fahma, F., Iwamoto, S., Hori, N., Iwata, T., & Takemura, A. (2010). Isolation preparation, and characterization of nanofibers from oil palm empty-fruit-bunch (OPEFB). *Cellulose, 17*, 977–985.
Fatah, I. Y., Khalil, H. P. S., Hossain, M. S., Aziz, A. A., Davoudpour, Y., Dungani, R., et al. (2014). Exploration of a chemo-mechanical technique for the isolation of nanofibrillated cellulosic fiber from oil palm empty fruit bunch as a reinforcing agent in composites materials. *Polymers, 6*, 2611–2624.

Fortunati, E., Puglia, D., Monti, M., Peponi, L., Santulli, C., Kenny, J. M., et al. (2013). Extraction of cellulose nanocrystals from Phormium tenax fibres. *Journal of Polymers and the Environment*, *21*, 319–328.

French, A. D. (2014). Idealized powder diffraction patterns for cellulose polymorphs. *Cellulose*, *21*, 885–896.

Han, J. Q., Zhou, C. J., French, A. D., Han, G. P., & Wu, Q. L. (2013). Characterization of cellulose II nanoparticles regenerated from 1-butyl-3-methylimidazolium chloride. *Carbohydrate Polymers*, *94*, 773–781.

Hassan, M. L., Bras, J., Hassan, E. A., Silard, C., & Mauret, E. (2014). Enzyme-assisted isolation of microfibrillated cellulose from date palm fruit stalks. *Industrial Crops and Products*, *55*, 102–108.

He, W., Jiang, X. C., Sun, F. W., & Xu, X. W. (2014). Extraction and characterization of cellulose nanofibers from Phyllostachys nidularia Munro via a combination of acid treatment and ultrasonication. *Bioresources*, *9*, 6876–6887.

Hideno, A., Abe, K., & Yano, H. (2014). Preparation using pectinase and characterization of nanofibers from orange peel waste in juice factories. *Journal of Food Science*, *79*, 1218–1224.

Jahan, M. S., Saeed, A., He, Z. B., & Ni, Y. H. (2011). Jute as raw material for the preparation of microcrystalline cellulose. *Cellulose*, *18*, 451–459.

Jang, J. H., Lee, S. H., Endo, T., & Kim, N. H. (2013). Characteristics of microfibrillated cellulosic fibers and paper sheets from Korean white pine. *Wood Science and Technology*, *47*, 925–937.

Jausovec, D., Vogrincic, R., & Kokol, V. (2015). Introduction of aldehyde vs. carboxylic groups to cellulose nanofibers using lccase/TEMPO mediated oxidation. *Carbohydrate Polymers*, *116*, 74–85.

Jiang, Z. H., Liu, Z. J., Fei, B. H., Cai, Z. Y., Yu, Y., & Liu, X. (2012). The pyrolysis characteristics of moso bamboo. *Journal of Analytical and Applied Pyrolysis*, *94*, 48–52.

Khalil, H. P. S. A., Bhat, A. H., & Yusra, A. F. I. (2012). Green composites from sustainable cellulose nanofibrils: a review. *Carbohydrate Polymers*, *87*, 963–979.

Khalil, H. P. S. A., Davoudpour, Y., Islam, M. N., Mustapha, A., Sudesh, K., Dungani, R., et al. (2014). Production and modification of nanofibrillated cellulose using various mechanical processes: a review. *Carbohydrate Polymers*, *99*, 649–665.

Khawas, P., & Deka, S. C. (2016). Isolation and characterization of cellulose nanofibers from culinary banana peel using high-intensity ultrasonication combined with chemical treatment. *Carbohydrate Polymers*, *137*, 608–616.

Li, M., Wang, L. J., Li, D., Cheng, Y. L., & Adhikari, B. (2014). Preparation and characterization of cellulose nanofibers from de-pectinated sugar beet pulp. *Carbohydrate Polymers*, *102*, 136–143.

Li, W., Zhang, Y. C., Li, J. H., Zhou, Y. J., Li, R. S., & Zhou, W. (2015). Characterization of cellulose from banana pseudo-stem by heterogeneous liquefaction. *Carbohydrate Polymers*, *132*, 513–519.

Lu, P., & Hsieh, Y. L. (2010). Preparation and properties of cellulose nanocrystals: rods spheres, and network. *Carbohydrate Polymers*, *82*, 329–336.

Lu, Q., Lin, W. Y., Tang, L. R., Wang, S. Q., Chen, X. R., & Huang, B. (2015). A mechanochemical approach to manufacturing bamboo cellulose nanocrystals. *Journal of Materials Science*, *50*, 611–619.

Lu, Q. L., Tang, L. R., Lin, F. C., Wang, S. Q., Chen, Y. D., Chen, X. R., et al. (2015). Preparation and characterization of cellulose nanocrystals via ultrasonication-assisted FeCl3-catalyzed hydrolysis. *Cellulose*, *21*, 3497–3506.

Ma, H. Y., Burger, C., Hsiao, B. S., & Chu, B. (2014). Fabrication and characterization of cellulose nanofiber based thin-film nanofibrous composite membranes. *Journal of Membrane Science*, *454*, 272–282.

Paakko, M., Ankerfors, M., Kosonen, H., Nykanen, A., Ahola, S., Osterberg, M., et al. (2007). Enzymatic hydrolysis combined with mechanical shearing and high-pressure homogenization for nanoscale cellulose fibrils and strong gels. *Biomacromolecules*, *8*, 1934–1941.

Pan, H., Shupe, T. F., & Hse, C. Y. (2007). Characterization of liquefied wood residues from different liquefaction conditions. *Journal of Applied Polymer Science*, *105*, 3739–3746.

Pang, C. H., Gaddipatti, S., Tucker, G., Lester, E., & Wu, T. (2014). Relationship between thermal behavior of lignocellulosic components and properties of biomass. *Bioresource Technology*, *172*, 312–320.

Pelissari, F. M., Sobral, P. J. A., & Menegalli, F. C. (2014). Isolation and characterization of cellulose nanofibers from banana peels. *Cellulose*, *21*, 417–432.

Qi, J. Q., Xie, J. L., Hse, C. Y., & Shupe, T. F. (2013). Analysis of Phyllostachys pubescens bamboo residues for liquefaction: chemical components, infrared spectroscopy, and thermogravimetry. *Bioresources*, *8*, 5644–5654.

Qing, Y., Cai, Z. Y., Wu, Y. Q., Yao, C. H., Wu, Q. L., & Li, X. J. (2015). Facile preparation of optically transparent and hydrophobic cellulose nanofibrils composite films. *Industrial Crops and Products*, *77*, 13–20.

Sacui, I. A., Nieuwendaal, R. C., Burnett, D. J., Stranick, S. J., Jorfi, M., Weder, C., et al. (2014). Comparison of the properties of cellulose nanocrystals and cellulose nanofibrils isolated from bacteria, tunicate, and wood processed using acid, enzymatic, mechanical, and oxidative methods. *ACS Applied Materials & Interfaces*, *6*, 6127–6138.

Shimizu, M., Saito, T., & Isogai, A. (2014). Bulky quaternary alkylammonium counterions enhance the nanodispersibility of 2,2,6,6-tetramethylpiperidine-1-oxyl-oxidized cellulose in diverse solvent. *Biomacromolecules*, *15*, 1904–1909.

Shinoda, R., Saito, T., Okita, Y., & Isogai, A. (2012). Relationship between length and degree of polymerization of TEMPO-Oxidized cellulose nanofibrils. *Biomacromolecules*, *13*, 842–849.

Silverio, H. A., Neto, W. P. F., Dantas, N. O., & Pasquini, D. (2013). Extraction and characterization of cellulose nanocrystals from corncob for application as reinforcing agent in nanocomposites. *Industrial Crops and Products*, *44*, 427–436.

Somerville, C., Bauer, S., Brininstool, G., Facette, M., Hamann, T., Milne, J., et al. (2004). Toward a systems approach to understanding plant cell walls. *Science*, *306*, 2206–2211.

Sun, F. B., & Chen, H. Z. (2008). Comparison of atmospheric aqueous glycerol and steam explosion pretreatments of wheat straw for enhanced enzymatic hydrolysis. *Journal of Chemical Technology and Biotechnology*, *83*, 707–714.

Sun, X. X., Wu, Q. L., Ren, S. X., & Lei, T. Z. (2015). Comparison of highly transparent all-cellulose nanopaper prepared using sulfuric acid and TEMPO-mediated oxidation methods. *Cellulose*, *22*, 1123–1133.

Takaichi, S., Saito, T., Tanaka, R., & Isogai, A. (2014). Improvement of nanodispersibility of oven-dried TEMPO-oxidized celluloses in water. *Cellulose*, *21*, 4093–4103.

Tang, Y. J., Yang, S. J., Zhang, N., & Zhang, J. H. (2014). Preparation and characterization of nanocrystalline cellulose via low-intensity ultrasonic-assisted sulfuric acid hydrolysis. *Cellulose*, *21*, 335–346.

Tibolla, H., Pelissari, F. M., & Menegalli, F. C. (2014). Cellulose nanofibers produced from banana peel by chemical and enzymatic treatment. *LWT—Food Science and Technology*, *59*, 1311–1318.

Wang, H. Y., Li, D. G., Yano, H., & Abe, K. (2014). Preparation of tough cellulose II nanofibers with high thermal stability from wood. *Cellulose*, *21*, 1505–1515.

Wu, Q., Meng, Y. J., Concha, K., Wang, S. Q., Li, Y. J., Ma, L. F., et al. (2013). Influence of temperature and humidity on nano-mechanical properties of cellulose nanocrystal films made from switchgrass and cotton. *Industrial Crops and Products*, *48*, 28–35.

Xie, J. L., Zhai, X. L., Hse, C. Y., Shupe, T. F., & Pan, H. (2015). Polyols from microwave liquefied bagasse and its application to rigid polyurethane foam. *Materials*, *8*, 8496–8509.

Xie, J. L., Hse, C. Y., Shupe, T. F., Qi, J. Q., & Pan, H. (2014). Liquefaction behaviors of bamboo residues in a glycerol-based solvent using microwave energy. *Journal of Applied Polymer Science*, http://dx.doi.org/10.1002/APP.40207

Xie, J. L., Huang, X. Y., Qi, J. Q., Hse, C. Y., & Shupe, T. F. (2014). Effect of anatomical characteristics and chemical components on microwave-assisted liquefaction of bamboo wastes. *Bioresources*, *9*, 231–240.

Xie, J. L., Qi, J. Q., Hse, C. Y., & Shupe, T. F. (2014). Effect of lignin derivatives in the bio-polyols from microwave liquefied bamboo on the properties of polyurethane foams. *Bioresources*, *9*, 578–588.

Yousefi, H., Faezipour, M., Hedjazi, S., Mousavi, M. M., Azusa, Y., & Heidari, A. H. (2013). Comparative study of paper and nanopaper properties prepared from bacterial cellulose nanofibers and fibers/ground cellulose nanofibers of canola straw. *Industrial Crops and Products*, *43*, 732–737.

Yue, Y. Y., Zhou, C. J., French, A. D., Xia, G., Han, G. P., Wang, Q. W., et al. (2012). Comparative properties of cellulose nano-crystals from native and mercerized cotton fibers. *Cellulose*, *19*, 1173–1187.

Yue, Y. Y., Han, J. Q., Han, G. P., Zhang, Q. G., French, A. D., & Wu, Q. L. (2015). Characterization of cellulose I/II hybrid fibers isolated from energycane bagasse during the delignification: morphology, crystallinity and percentage estimation. *Carbohydrate Polymers*, *133*, 438–447.

Zhang, H. R., Pang, H., Shi, J. Z., Fu, T. Z., & Liao, B. (2012). Investigation of liquefied wood residue based on cellulose, hemicellulose, and lignin. *Journal of Applied Polymer Science*, *123*, 850–856.

Zhu, J. Y., Sabo, R., & Luo, X. L. (2011). Integrated production of nano-fibrillated cellulose and cellulosic biofuel (ethanol) by enzymatic fractionation of wood fibers. *Green Chemistry*, *13*, 1339–1344.